

B.S. Thesis for Research Distinction in Chemical Engineering

CO₂ Assisted Impregnation of Electrospun Polymer Blends for Biomedical Applications

Submitted to:

The Engineering Honors Committee

122 Hitchcock Hall

College of Engineering

The Ohio State University

Columbus, Ohio 43210

By

Prathamesh S. Karandikar

Research Advisor: David L. Tomasko

Chemical and Biomolecular Engineering

Koffolt Laboratories 140 W 19th Avenue

The Ohio State University

Columbus, Ohio 43210

July 12th, 2013

Table of Contents

1.	Introduction	1
2.	Literature Review.....	3
3.	Materials and Methods.....	8
4.	Results and Discussion.....	13
5.	Conclusions.....	35
6.	Recommendations for Future Work.....	37
7.	Acknowledgments.....	38
8.	References.....	39

List of Figures

Figure 1: SEM image of As spun A) Tri PMMA B) Tri PCL C) Tri Gelatin blends	13
Figure 2: Average fiber diameter of ternary blend electrospun fibers.....	14
Figure 3: SEM images of electrospun fibers post supercritical CO ₂ exposure A) TriPMMA B)TriPCL C)TriGelatin.....	14
Figure 4: SEM images of electrospun fibers following 100% ethanol treatment A) Tri PCL B) TriGelatin C)TriPMMA.....	15
Figure 5: Average fiber diameter of ternary blend electrospun fibers post ethanol treatment.....	16
Figure 6: Modulus of electrospun fiber dog bones.....	17
Figure 7: % Elongation of electrospun fiber dog bones.....	18
Figure 8: Stress vs % Elongation curves for ternary blends and pure components.....	20
Figure 9: UTS of electrospun fiber dog bones.....	21
Figure 10: DSC scans of ternary blends as-spun and after supercritical CO ₂ (8.27 MPa and 37°C) treatment. Image (A) Tri-PCL (B) Tri-Gelatin (C) Tri-PMMA.	24
Figure 11: XRD patterns of pure PCL, PMMA and gelatin along with ternary blends before and after CO ₂ exposure.....	25
Figure 12: Cumulative release curves of ternary blends under different impregnation conditions A) Tri-Gelatin B) Tri-PCL C) Tri-PMMA D) Adsorption E) Subcritical CO ₂ F) Supercritical CO ₂	28

Figure 13: Comparison of % dye release profiles from ternary blends after different impregnation conditions for initial 5 days of release.....	32
Figure 14: Degradation of ternary electrospun scaffolds in PBS release medium.....	33
Figure 15: SEM images of as-spun ternary blends after 24 hour of degradation in PBS (A) Tri-PCL (B) Tri-Gelatin (C) Tri-PMMA.....	34

List of Tables

Table 1: Diffusion coefficients of Rhodamine B from ternary blends infused using different impregnation conditions in a static release medium (PBS).....	34
--	----

1. Introduction:

The use of CO₂ as polymer processing agent became popular in the mid 1990's. Colton and Suh reported one of the first uses of CO₂ as a foaming agent for polystyrene in 1987¹. Since then CO₂ has been utilized successfully as solvent, anti-solvent or plasticizer in polymer processing such as polymer modification, polymer composites, polymer blending, microcellular foaming, particle production and polymer synthesis^{2, 3}. Its use as a supercritical fluid, along with its plasticizing and solvent properties, has enabled it to be used in a wide variety of tissue engineering and regenerative medicine applications⁴⁻⁹. CO₂ induced plasticization arises due to Lewis acid-base interactions^{10, 11}. These interactions result in sorption of CO₂ in the polymer matrix, allowing for the basis of CO₂ assisted impregnation of polymers. CO₂ has a number of advantages for polymer processing in tissue engineering, including its ease of use, low cost, and the opportunity to circumvent the use of organic solvents.

The focus of this project is on the use of supercritical and subcritical CO₂ for the processing of electrospun polymer scaffolds for potential tissue engineering and drug delivery devices. Electro spinning is a novel, emergent technique to develop 3D, nanoscale matrices for tissue engineering. Utilizing a high-voltage power supply to generate strong electric fields, polymer solutions are drawn out of needle tips and strained into nano-diameter, non-woven fiber mats. The formation of fibers is achieved due to tangential stresses and bending instabilities^{12, 13}. The diameter of the viscoelastic jet can be reduced to produce micron and nano-sized fibers by using the electrostatic repulsions between the surface charges¹⁴. Post fabrication processing of electrospun polymers is essential to their application. By blending different biocompatible polymers the mechanical and microstructural properties of the scaffold can be tailored to the application. Post-fabrication processing of electrospun polymer scaffolds is also essential to

adding biofunctionalization and added cellular in-growth characteristics. Direct electrospinning of polymer solutions with additives presents some problems. Encapsulation of a bioactive molecule using supercritical CO₂ helps to protect conformational sensitivity molecules from the shear forces present during the electrospinning process¹⁴.

An inexpensive and gentle method is required to infuse these biomolecules while preserving their activity and controlling their release. CO₂ can be used as a swelling agent for polymers and can help impregnate the scaffolds with desirable additives such as drugs or bioactive compounds^{15,16}. Recently, the post-processing of novel electrospun PCL-Gelatin nano fiber blends using supercritical CO₂ was investigated. The PCL-Gelatin nanofibers displayed resilience to microstructure deformation under exposure to SCCO₂, furthermore different conditions of high pressure CO₂, showed different loading and release profiles¹⁷. This has set a precedent to exploring controlled release applications using electrospun fibers as substrates for CO₂ impregnation. In order to further explore the effects of blend composition on the impregnation and release characteristics of electrospun fibers different biocompatible blends of PMMA, PCL and Gelatin were explored. It is hypothesized that by incorporating an amorphous polymer such as PMMA, the blend will be more responsive to swelling agents and elicit higher additive loading¹⁸. An additional synthetic component will also allow access to a greater range of physical and chemical properties, and help optimize scaffold characteristics in a predictable manner.

The objective of this thesis is to perform a detailed characterization of electrospun polymer blends derived from biocompatible polymers by determining their temperament to exposure to different high pressure CO₂ infusion treatments. The characterization was based on mechanical

properties, microstructural analysis and resilience of the fibers to various impregnation and release conditions.

2. Literature Review:

Currently, biomedical engineering is tackling challenges in the development of controlled drug delivery and tissue engineered scaffolds due to lack of cellular response, mechanical instability and *in vivo* degradation of these systems¹⁹. Electrospun polymer fibers have been used in controlled drug delivery systems to achieve high surface area, porosity and simplicity of the process^{20,21}. Tissue engineering is an interdisciplinary field which deals with the repair and regeneration of damaged tissues. One aspect of tissue engineering is the development of implantable scaffolds with specific mechanical and biological properties that can mimic extracellular matrix (ECM). An implantable scaffold needs to provide an environment for cells to grow and proliferate in order to regenerate tissue²². Electrospinning provides 3D porous structures which aid in mimicking ECM. The efficacy of such scaffolds is based on several interaction parameters such as cellular adhesion, proliferation, biocompatibility in addition to scaffold characteristics like structural integrity, void volume and fiber diameter^{23, 24}. Design of an efficient scaffold is a complex process due to simultaneous optimization of above factors.

Biocompatible polymers have received significant attention due to their wide range of application in tissue engineering and controlled drug release systems²⁵. Poly-caprolactone (PCL) is one of the most widely used synthetic polymers which is semi-crystalline, biocompatible and biodegradable. An extended degradation period (about 24 months) makes PCL an ideal candidate for long term *in vivo* applications²⁶⁻²⁸. PCL is an attractive option for tissue engineered implants due to its outstanding elastomeric properties²⁹. It is well known in literature to fabricate

electrospun PCL scaffolds with random or aligned fiber morphology. Electrospun PCL based scaffolds have been used as prosthetics for blood vessels and nerve cell proliferation^{30, 31}. Polymethyl methacrylate (PMMA) is a synthetic, non-degradable biocompatible polymer which is primarily used in bone repair and hard tissue regeneration^{32, 33}. PMMA based tissue engineered scaffolds have demonstrated good cellular adhesion, proliferation, and viability³⁴. Electrospun PMMA fibers have been prepared to form 3-D tissue engineered scaffolds and have been tested *in vitro* and *in vivo* applications^{35, 36}. PMMA has also been used in making medical devices, controlled drug delivery systems and regenerative medicines^{23, 37}. Although, PMMA has high compressive strength, it is brittle and characterized by low tensile strength and fails to fulfill mechanical strength requirements that are essential for certain implantable scaffolds. Bio-functionality of a scaffold is essential for achieve efficient cell adhesion and proliferation. A scaffold is functionalized by incorporating bioactive agents in the bulk or on the surface of the scaffold. A functionalized scaffold has active sites that can be recognized by cells and enhance cell attachment³⁸. It has been shown that use of active molecules derived from natural ECM proteins is a better way to produce functionalized scaffolds. For instance, incorporation of gelatin, which is a biodegradable, natural protein, in the 3D Poly-l-lactic acid scaffold, indicated better cellular adhesion and proliferation of MC3T3-E1 as compared to the control^{39, 40}.

Synthetic polymers have chemical stability, ease of processability, robustness and consistent control over fabrication parameters, mechanical properties and morphology of resulting scaffolds. However, they lack, surface recognition sites for cellular affinity and are characterized by hydrophobic nature⁴¹. Cellular adhesion is dependent on both physical and chemical characteristics of the scaffold⁴². It depends on receptor mediated and non-receptor mediated

interactions between cells and the scaffold. Non receptor mediated interactions facilitate cell adhesion through weaker chemical interaction such as hydrogen bonding and charged interactions between functional groups of the scaffolds and cells. These forces can be fine-tuned in synthetic polymers but are not enough to elicit cellular adhesion. Receptor mediated interactions on the other hand are elicited by ECM molecules such as collagen, elastin, gelatin to which cells bind through binding proteins⁴³. Natural polymers have an advantage in harnessing such interactions for cell proliferation. However, electrospun scaffolds made purely from natural ECM proteins are characterized by rapid hydrolysis in aqueous media and present a need for crosslinking to be functional⁴⁴. Several researchers are looking to blend natural and synthetic polymers to explore properties of such composites in biomedical applications and overcome the limitations of purely synthetic and natural polymer based scaffolds for tissue engineering⁴⁵⁻⁴⁸. Adjusting compositions of such blends gives precise control on properties on the blends. For instance, controlled degradation of scaffolds was achieved using PAA/PTMC scaffolds⁴⁹. Here degradation was regulated by adjusting the fast degrading PAA component for in-vivo implants. This aspect is crucial in application where scaffold degradation rates must be tailored to match tissue regeneration rate⁵⁰. Moreover blending of certain natural and synthetic polymers in the same solvent system permits the formation of constructs that are stable in aqueous environment⁵¹ as is demonstrated by several gelatin based hydrogels. This helps to bypass the need for crosslinking and thus preserves biocompatibility. Blending polymers in general allows access to greater range of physical, chemical and mechanical properties while also opening new avenues to polymer processing. There are several studies on blends of gelatin with synthetic polymers for tissue engineering applications and these have proven to perform better than their pure synthetic counterparts^{30, 52-62}. Gelatin acts as a “biological cue⁶³” for cells and provides better

biocompatibility than a synthetic polymer. Gelatin may also counteract the hydrophobic nature of some synthetic polymers which is an added advantage for applications that require aqueous environments. There is also evidence to suggest that biomolecules delivered using gelatin based controlled release devices tend to persist in bioactivity⁶⁴.

Post-fabrication processing of tissue engineered scaffolds and drug delivery systems is challenging as physical and chemical characteristics of these systems need to be preserved during processing. High temperatures and organic solvents are avoided due to concerns about their toxicity and damage to sensitive polymers. Supercritical fluids (SCF) have easily tunable physical properties (e.g density, viscosity etc) which are useful in the wide range of applications⁶⁵. Carbon dioxide (CO₂) is one of the most popular SCF due to its benign critical point conditions (7.38 MPa at 31.1 °C). Recent studies have explored potential of CO₂ for sustainable and inexpensive processing of many polymers for foaming, sterilization, solvent extraction and impregnation^{66, 67}. CO₂ has specific molecular interactions with many polymers which result in altered polymer properties to ease plasticization of polymer⁶⁸. In the presence of CO₂, properties of many polymers (such as glass transition temperature T_g etc.) are significantly different than those of pure polymer and can be tuned by adjusting CO₂ pressure and temperature⁶⁹. CO₂ offers a green alternative way for impregnation of drugs and biomolecules in the polymer substrate. Various studies have already studied plasticization and impregnation of PCL and PMMA in the presence of high pressure CO₂^{70, 71}. Although subcritical gaseous CO₂ can reversibly swell PCL during impregnation, it results in fast release of the impregnated additive due to low solubility of additive in dense CO₂. Liquid CO₂ can swell pure PCL reversibly without permanent deformation but it has low diffusivity. Supercritical CO₂ (SCCO₂)

has moderate diffusivity in polymers and adequate solubility for an additive compared to that of dense gas and liquid CO₂. However, if PCL is subjected to SCCO₂, it melts and loses mechanical integrity⁷². Similarly PMMA shows an irreversible change in the structure if processed under certain SCCO₂ conditions⁷³. The structure of a scaffold (porosity of foams and fiber structure for fibrous scaffold) is an essential factor for cell proliferation. In our recent work we showed that if PCL is blended with gelatin the resulting blend has distinct properties. When subjected to high pressure CO₂, the blend can be swelled reversibly by dense, liquid and SCCO₂¹⁷. Our recent results have confirmed that pure PCL swells under high pressure CO₂ whereas pure gelatin compresses due to dehydration in the presence of CO₂. Simultaneous swelling of PCL and shrinking of gelatin stabilize the blend under SCCO₂ without deformation. This discovery has opened an avenue to explore CO₂ assisted impregnation of biocompatible blends with gelatin for drug delivery and tissue engineering.

In this thesis, we have explored the properties of PMMA-PCL-gelatin ternary blend for biomedical applications. Different compositions of ternary blends have been investigated to prepare electrospun scaffolds. Adjusting ratio of the blend components allows control over mechanical properties and degradation rate of the scaffolds. High pressure CO₂ assisted impregnation was used to impregnate Rhodamine B dye in these scaffolds. Release profiles of the dye from these scaffolds were studied over specific period of time. Results indicate the PMMA-PCL-gelatin ternary blends have promising properties for various biomedical applications.

3. Materials and Methods:

3.1 Electrospinning

5 % w/w polycaprolactone (PCL) (M_n 70,000-90,000; Sigma-Aldrich, St. Louis, MO), 3% polymethyl methacrylate (PMMA) (M_n 350,000; Sigma-Aldrich, St. Louis, MO) and 6.7 % w/w porcine gelatin type A (300 Bloom; Sigma-Aldrich, St. Louis, MO) solutions were prepared in 1,1,1,3,3,3-hexafluoro-2-propanol (HFP) (> 99% purity; Sigma-Aldrich, St. Louis, MO) stirring at room temperature ($\cong 25^\circ\text{C}$) for 24 hours. Weight % concentrations were chosen based on electrospinning of pure polymer to achieve required fiber morphology. Different compositions of ternary blends are obtained on volume/volume basis by adjusting volume of each component in the blend solution. After complete mixing of solutions Tri-PCL (PCL 50%, PMMA 25%, Gelatin 25%), Tri-PMMA (PCL 25%, PMMA 50%, Gelatin 25%) and Tri-Gelatin (PCL 25%, PMMA 25%, Gelatin 50%) blends were then poured individually into separate 20cc syringes, fitted with a 20 gauge blunt tip needle, and electrospun using a DC high voltage power supply (Glassman High Voltage, Inc., High Bridge, NJ) at positive 20 kV, 20 cm needle-to-collector distance, 10 mL/hr flow rate, for 45-60 min. 8 cm x 8 cm randomly oriented electrospun fiber mats of Tri-PCL, Tri-PMMA and Tri-Gelatin were produced on aluminum non-stick foil. The as-spun mats were then placed in a vacuum oven (< 30 mmHg) at 25°C for 24 hours to remove any residual HFP solvent. The mats were then cut into 13 mm diameter discs using a metal punch with an approximate fiber mat weight of 15 mg (Arch Punch; C.S. Osborne & Co, Harrison, N.J.) and stored at ambient room conditions until future use.

3.2 Scanning Electron Microscopy (SEM)

SEM (Quanta 300, Netherlands and JEOL JSM-5500, USA) was used to characterize surface morphology and microstructure of the blended electrospun mats. Samples were mounted on aluminum stubs, covered with carbon adhesive tape (Ted Pella, Reading, CA), and sputter coated with Au (Pelco Model 3 sputter coater 91000, USA) at an emission current of 15 mAmps, under Argon atmosphere for 60 sec to achieve an approximately 15 nm thick layer. Coated samples were then analyzed using an accelerating voltage of 5 kV for micro-structural and morphological characteristics of the electrospun fibers. Image analysis was carried out using ImageJ software.

3.3 Differential Scanning Calorimetry (DSC)

DSC analysis of electrospun mats were carried out in a TA instruments DSC Q 100. All test runs were performed under nitrogen purging at 50 ml/min. Thermal properties were investigated for all the blends. All samples were analyzed in their pure form and after treatment with supercritical CO₂. In the case of CO₂ treatment, fibers were pretreated with supercritical CO₂ (8.27 MPa and 37°C) for 2 hours. All samples (10mg in weight) were equilibrated at -10°C and heated to 160°C at 10°C/min. After maintaining isothermal conditions at 160°C for 1 min, samples were cooled to -10°C at 10°C/min to finish cycle. TA instruments universal analysis software was used to analyze DSC scans.

3.4 X-ray Diffraction (XRD)

XRD patterns were obtained for as-spun PCL, gelatin, and PMMA nanofiber scaffolds as a baseline for analysis, and in addition XRD profiles for each of the as-spun tri-blends (Tri-PMMA, Tri-Gelatin, and Tri-PCL) were acquired using a Rigaku Ultima-III diffractometer (Rigaku Ultima-III, Rigaku Corp., USA) operated in Bragg Brentano mode. The X-ray source was a Cu-K_α and a diffracted beam monochromator was used. Electrospun specimens were mounted on aluminum disks using tape to ensure the sample was flat. Sample thickness was

measured before XRD to provide consistency from sample to sample. The disks were rotated at 120 rpm during data acquisition with a step-size 0.04° over the range of 19 to $25^\circ 2\theta$ and the integration time at each step was 24 seconds. A constant linear background was used in the profile fitting to eliminate potential background noise and scattering when comparing the patterns from different samples. All XRD pattern analysis was performed using JADE software (MDI, v 8.1).

3.5 Mechanical Testing

The mechanical properties of the as-spun electrospun scaffolds were determined using a uniaxial bench-top testing machine (TEST RESOURCES- Type R, TestResources Inc, Shakopee, MN). The scaffolds of pure PMMA, pure PCL, Pure gelatin and blended PMMA-PCL-Gel fibers were tested to analyze mechanical properties. Samples were cut to a gage-length of 20 mm and gage-width of 2.4 mm by placing the fiber mats between two 2 mm thick stainless steel ‘dog-bone’ shaped templates. A stainless-steel surgical blade was employed to make the straight cuts of the template, and a 6-mm dermal biopsy punch was used to cut the radii. Great care was taken to insure clean-cut samples, reducing sample flaws that could result in inaccurate testing. Placing the gage-length of the ‘dog bone’ shaped samples between two glass-slides and measuring the thickness of the sample using a digital micrometer determined sample thickness. Five samples from each of the different groups were analyzed. Samples were placed into aluminum grips and pulled at a cross-head speed of 5 mm/min by a 222.5 N load cell to failure. Force as a function of displacement was recorded and converted for engineering-stress vs. elongation analysis.

3.6 Infusion and Release

The 13 mm diameter electrospun discs of all three combinations were weighed (Ohaus galaxy 100, NJ, USA) and placed in 24 well plate. 100 μ L of 1 mg/mL Rhodamine B (Standard Fluka;

Sigma-Aldrich, St. Louis, MO) in ethanol (>99.5% purity, 200 Proof; Sigma-Aldrich, St. Louis, MO) solution was placed uniformly onto each of the scaffolds. These scaffolds were placed in chemical hood to dry for 2 hours until all the ethanol was evaporated. Scaffolds were moved using tweezers in order to avoid their adhesion to the well plate surface. In the case of adsorption-only study, scaffolds were washed 3 times with pure ethanol after 30 min. For CO₂ infusion, dried scaffolds were then placed into a high pressure stainless steel vessel. Temperature of the vessel was controlled using heat tape and monitored using a temperature sensor (Omega CSC 32, Stamford, CT, USA). Bone-dry CO₂ (99.9% purity, Praxair, Columbus, OH) was allowed to flow in the pressure vessel and pressure was controlled with the syringe pump (500 D; Teledyne ISCO, Inc., Lincoln, NE). Equilibrium conditions were maintained for 2 hours. Subcritical CO₂ infusion was conducted at 6.20 MPa and 25°C whereas supercritical CO₂ conditions were maintained at 8.27MPa and 37°C. In either case, pressure was released by reversing syringe pump slowly (0.5-1 ml/min) over >12 hours. Scaffolds were then washed with pure ethanol 3 times and dried in the chemical hood. Rhodamine B release was carried out in 24 well plates for all three impregnation conditions (adsorption, subcritical CO₂ and supercritical CO₂) by immersing each scaffold in the 2 ml of phosphate buffer saline (PBS) and keeping it in the incubator (Wiseven, Witeg Labortechnik GmbH, Germany) at 37°C. At each time point, 2 aliquots were taken from each sample and stored in 96 well plates. PBS was replaced with fresh PBS in each well after every time point. All 96 well plates containing aliquots were stored in the refrigerator. A UV-vis 96-well plate spectrometer (Spectra Max 190 Absorbance UV-VIS plate reader, Sunnyvale, CA) was used to measure the absorbance of released Rhodamine B solutions at a wavelength of 535 nm. Spectrometer readings were then converted to concentration values

($\mu\text{g/mL}$) using a polynomial calibration curve produced by making serial dilutions of Rhodamine B in PBS. Statistical analysis was carried using JMP software.

3.7 Weight loss Study:

Similar to the infusion study, 13 mm diameter discs of Tri-PMMA, Tri-PCL and Tri-Gelatin fibers were weighed and placed in 24 well plates. Each scaffold was immersed in 2 ml of PBS and stored in the incubator (Wiseven, Witeg Labortechnik GmbH, Germany) at 37 °C. Scaffolds were then removed after specific time interval to wash with distilled water in order to get rid of salts. These scaffolds were then dried overnight in a vacuum oven to remove all water before they were weighed again to analyze weight loss.

4. Results and Discussion:

4.1 Polymer Blend Characterisation

PCL- Gelatin blends were previously determined to be successful candidates for CO₂ based infusion. The success was determined based on the resilience of the blend to Supercritical CO₂ exposure. In order to enhance impregnation capabilities PMMA was added to the blend. Figure 1 depicts the as spun ternary blends.

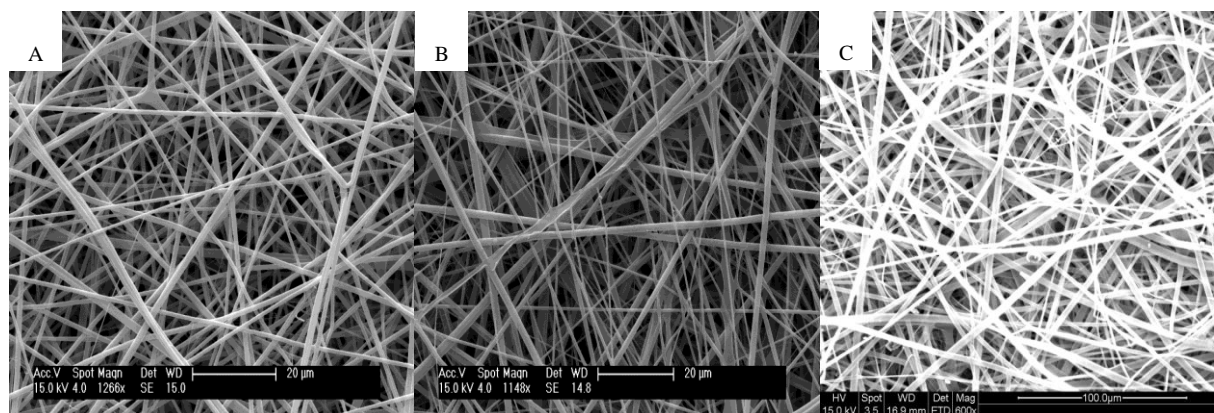


Figure 1: SEM image of as spun A) Tri-PMMA B) Tri-PCL C) Tri-Gelatin blends

All three compositions explored in this study show fibers in the range of diameters 0.75-1 μm. Tri-Gelatin scaffolds have flat ribbon like fiber morphology with large fiber diameter⁷⁴ due to higher percentage of gelatin in the blend. Tri-PCL and Tri-PMMA fibers have well defined cylindrical structure and uniform fiber diameter. The fiber diameter of the individual blends is displayed in Figure 2.

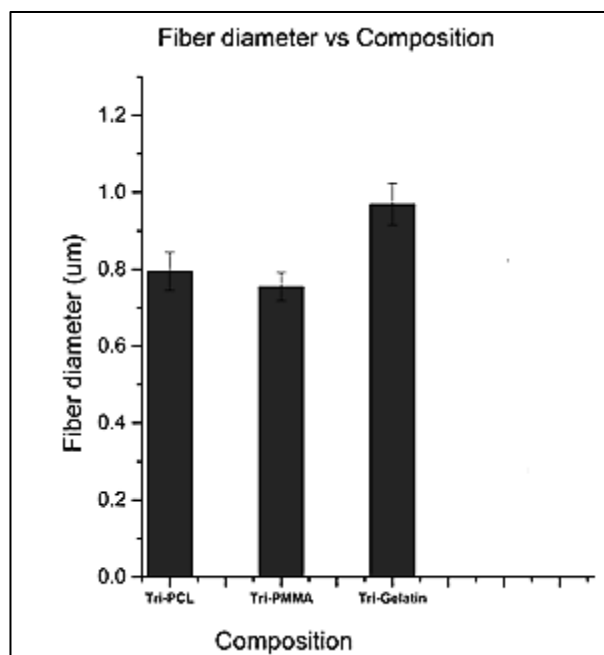


Figure 2: Average fiber diameter of ternary blend electrospun fibers

In order for the scaffolds to be viable for CO₂ infusion of additives, it is essential that electrospun fibers maintain their microstructure during the processing stage. Figure 3 shows the SEM image of ternary blends post supercritical CO₂ exposure at 8.27MPa and 37°C.

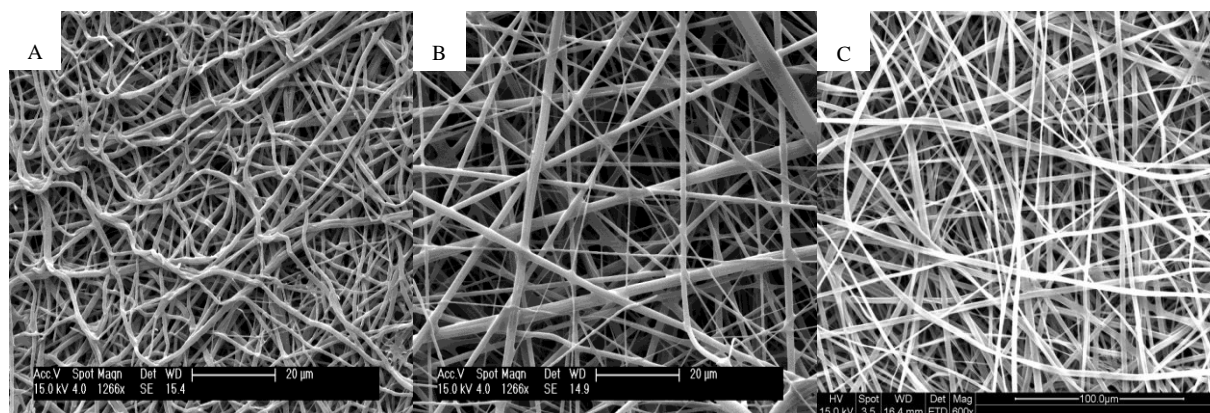


Figure 3: SEM images of electrospun fibers post supercritical CO₂ exposure A) Tri-PMMA

B) Tri-PCL C) Tri-Gelatin

Although Tri-PMMA blend shows no deformation of fibers, stress relaxation of fibers causes a reduction in the porosity of the scaffold (Figure 3A). Stress relaxation of Tri-PMMA fibers change scaffold morphology into wormlike structure. There is no notable change in the morphology for Tri-Gelatin fibers (Figure 3C). Tri-PCL scaffolds show fiber melting and fusion of fiber at all the fiber junctions; nonetheless fiber structure and inter-fiber porosity is maintained after supercritical CO₂ exposure.

In the infusion process, the initial loading was made using an ethanol solution of the additive Rhodamine -B. To study the effect of the initial loading on fiber morphology the as spun fibers were exposed to 100% ethanol for 30 minutes. The scaffolds were then dried and imaged using SEM. Figure 4 depicts the resulting SEM image after ethanol treatment.

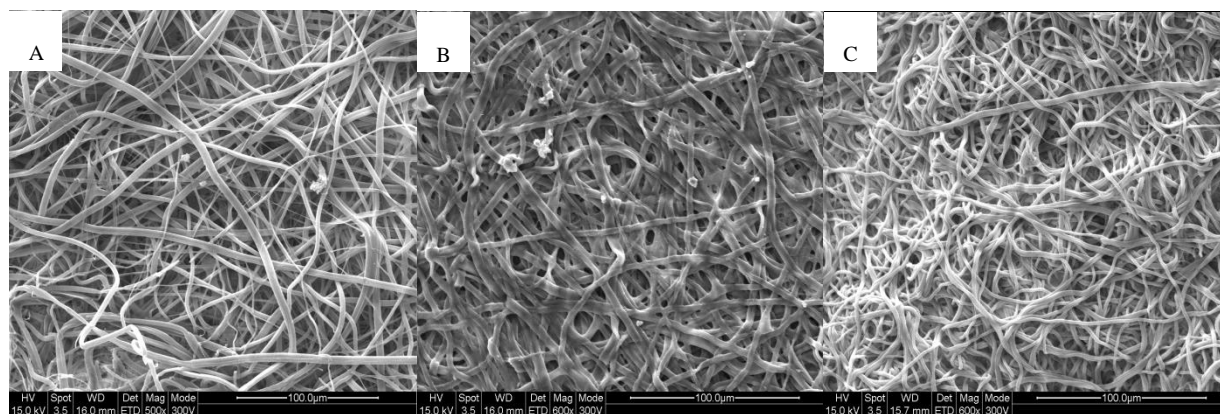


Figure 4: SEM images of electrospun fibers following 100% ethanol treatment A) Tri-PCL

B) Tri-Gelatin C)Tri-PMMA

Fiber diameter analysis shows no significant change in diameter of Tri-PCL. Tri-PCL fibers show no noteworthy change in fiber structure and void volume of scaffolds. Tri-Gelatin and Tri-PMMA scaffolds show significant change in void volume and fiber morphology after ethanol

treatment. There is a notable increase in Tri-Gelatin and Tri-PMMA fiber diameter due to ethanol treatment. Tri-Gelatin blend shows deformation of fiber structure, with some evidence of fiber melting along with a reduction of void volume. Although Tri-PMMA blend shows no deformation of fibers, stress relaxation of fibers causes a reduction in the porosity of the scaffold. Stress relaxation of Tri-PMMA fibers change scaffold morphology into wormlike structure. The fiber diameters post ethanol treatment were measured and presented in Figure 5.

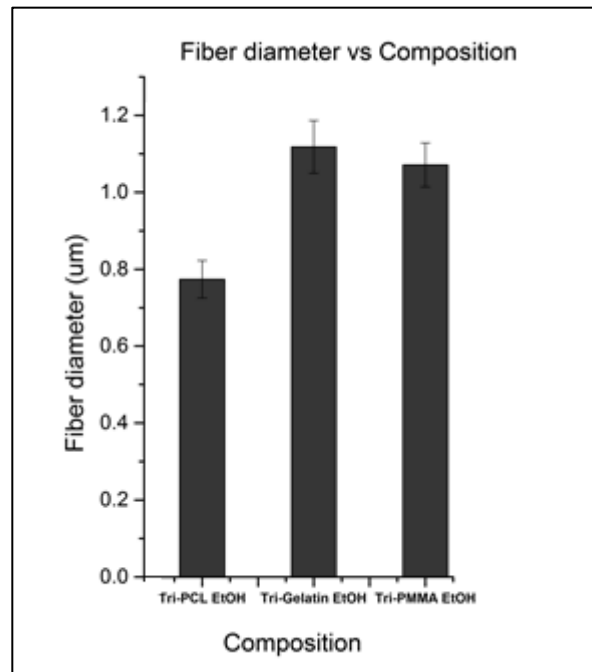


Figure 5: Average fiber diameter of ternary blend electrospun fibers post ethanol treatment

4.2 Mechanical Characterization of Electrospun fibers

Blend composition of polymer solution has a significant impact on the mechanical properties of the electrospun scaffolds. In order to characterize the effect of blend components on mechanical properties, the modulus, % elongation and ultimate tensile strength of the electrospun scaffolds was measured for each of the ternary blends and compared to their pure components.

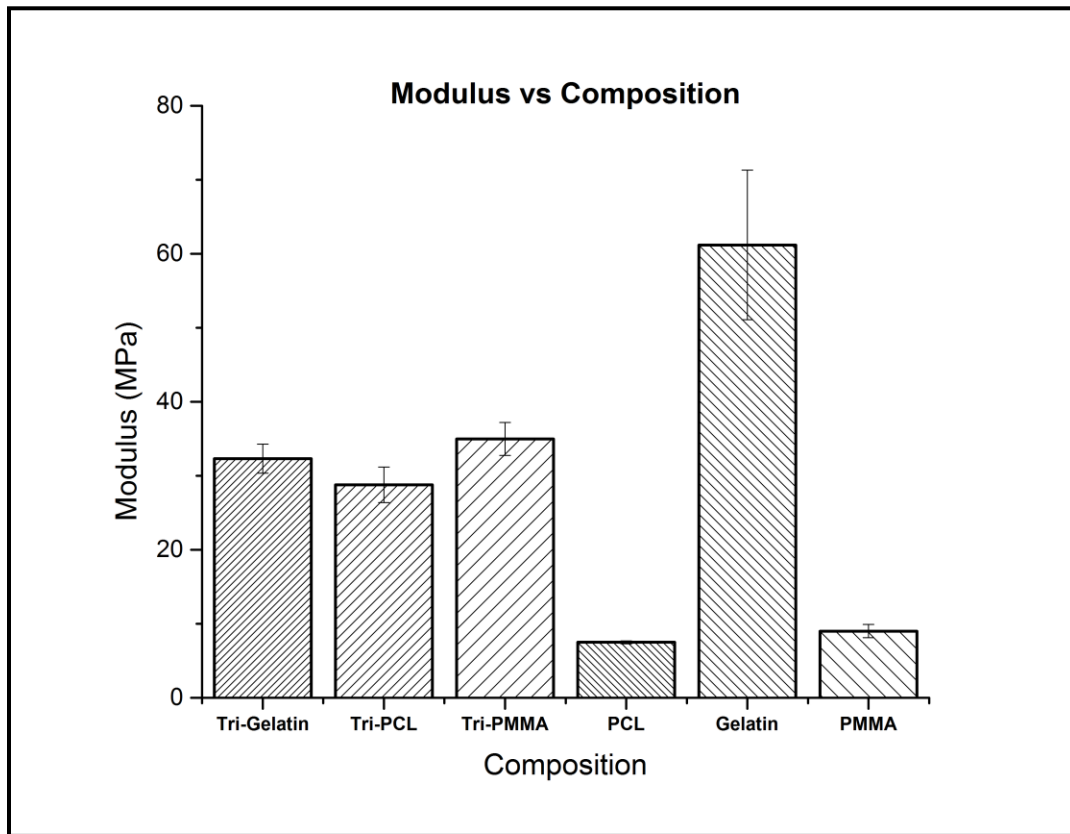


Figure 6: Modulus of electrospun fiber dog bones

Figure 6 represents the modulus of the electrospun fibers obtained by calculating the slope of the linear region of the stress vs. strain curve. As is evident pure form PCL and PMMA fibers are not strong and offer little resistance to deformation. Incorporation of gelatin helps increase the modulus of the ternary blends of PCL and PMMA significantly. Higher modulus is critical for

tissue engineering applications that require resistance to deformation at the site of implantation. The reduced modulus of Tri Gelatin can be attributed to the addition of PMMA and PCL. Figure 7 displays the % elongation of the ternary blends as compared to the pure components. While all ternary blends have similar modulus as attested in Figure 6, they vary significantly as to the amount of elongation they undergo until their break point. Each polymer blend shows an increase in the elongation when compared to its dominant pure form. PCL shows almost a 2 fold increase in elongation in Tri-PCL blend whereas PMMA and gelatin shows almost 8 times increase when they are in blended form.

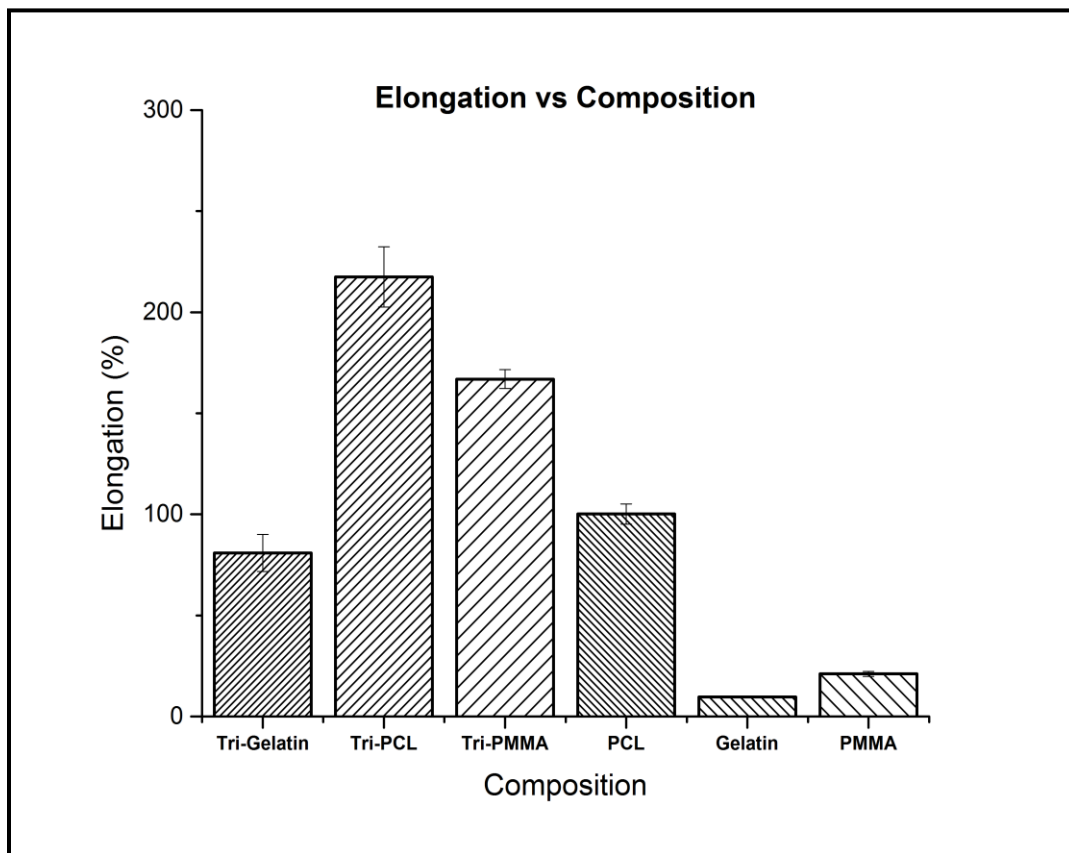


Figure 7: % Elongation of electrospun fiber dog bones

Finally ultimate tensile strength of the scaffolds was determined. The ultimate tensile strength (UTS) is the maximum engineering stress level reached in a tension test. In brittle materials, the UTS is reached at the end of the linear-elastic portion of the stress-strain curve or close to the elastic limit. In ductile materials, the UTS is well outside of the elastic portion of the stress strain curve into the plastic portion of the stress-strain curve. The raw data gathered from the stress tests on five representative samples of each ternary blend and pure component is depicted in Figure 8. All ternary blends have a ductile nature. Moreover the dramatic augmentation of mechanical properties is evident. Pure gelatin represents typical brittle failure with high modulus, but the sample can absorb very little energy before failure. Similarly pure PMMA undergoes very limited elongation before brittle failure. However, in their blended form both tri-PMMA and tri-gelatin show significant increase in % elongation at maximum stress. This can be characterized as increased toughness of the polymer. Figure 9 shows the UTS values achieved by different scaffolds during mechanical testing.

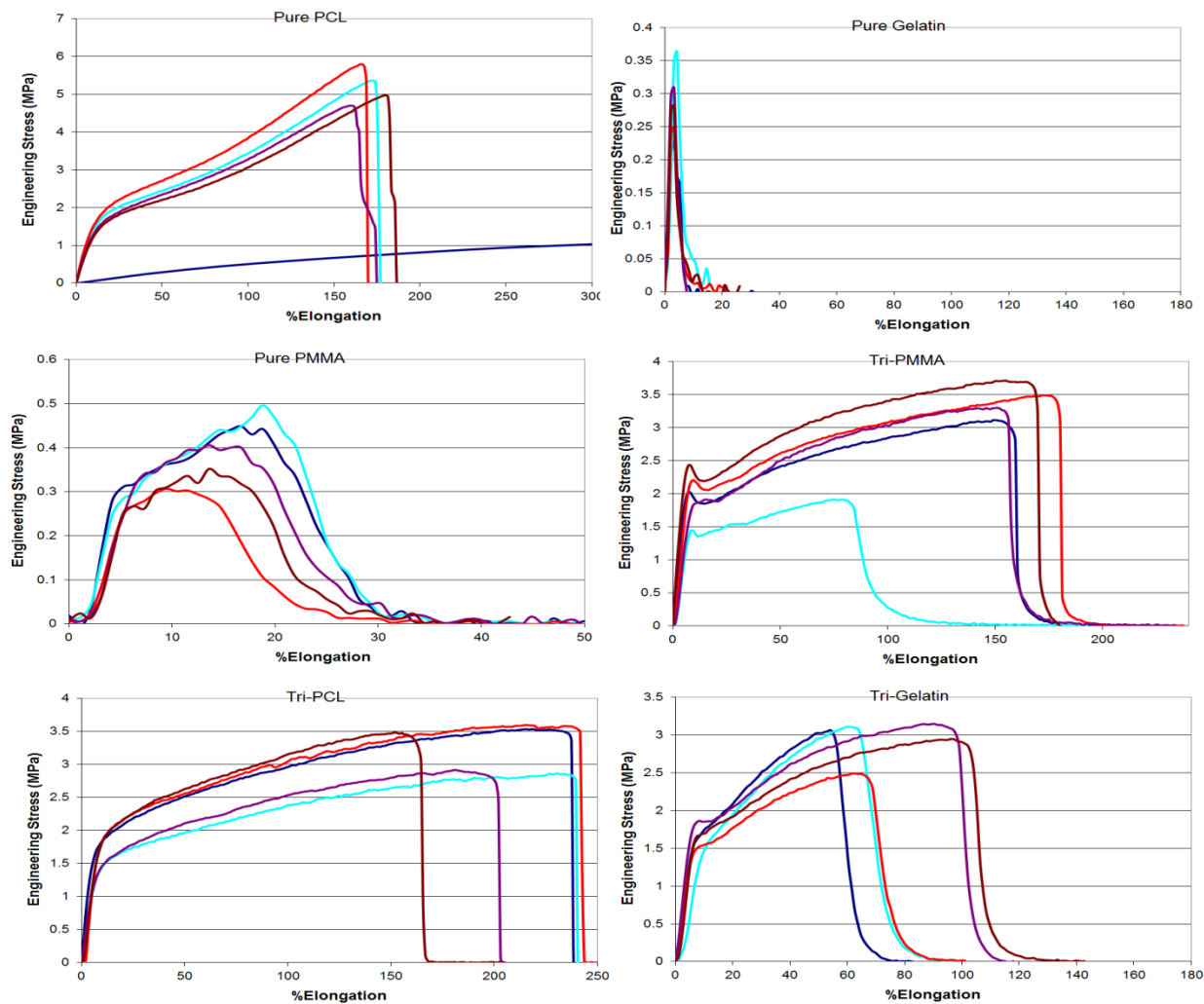


Figure 8: Stress vs % Elongation curves for ternary blends and pure components

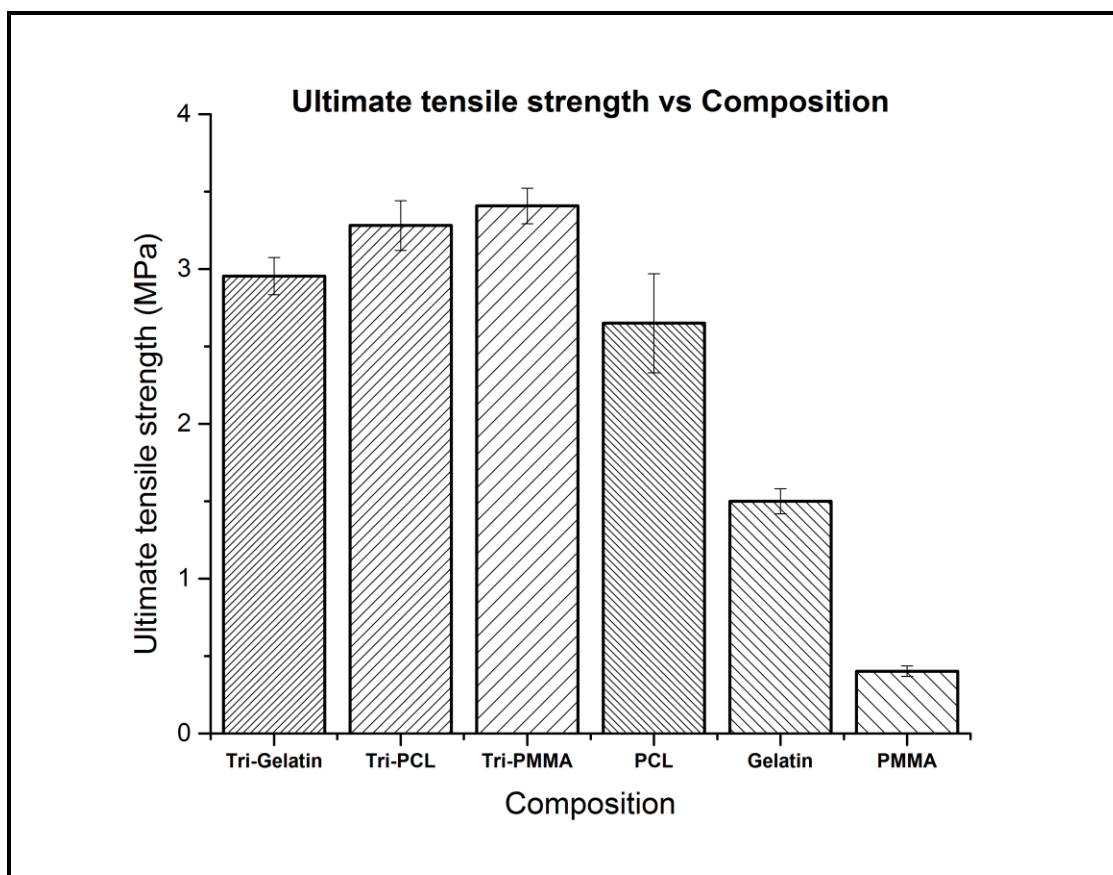


Figure 9: UTS of electrospun fiber dog bones

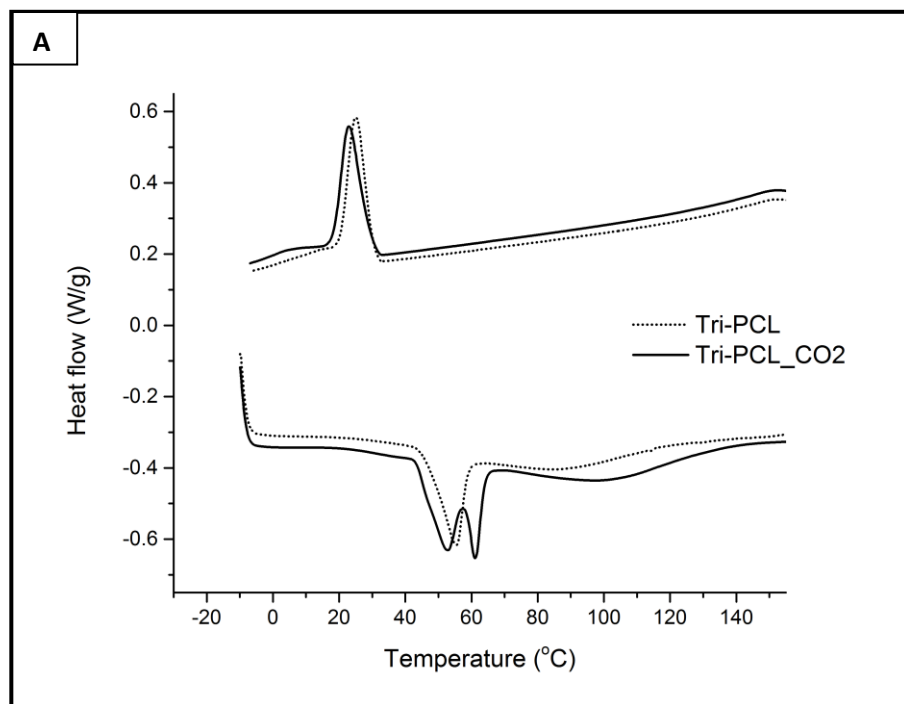
There is notable enhancement in the UTS of Tri-PMMA and Tri-Gelatin blends when evaluated against their pure states. Although Tri-PCL blend shows some improvement over pure PCL it is not as high as PMMA and gelatin. This study was designed to manipulate the mechanical properties of the blend by adjusting the composition in order to make tissue engineered scaffolds or drug delivery systems for different applications. Mechanical testing results show that there is a remarkable change in the properties of the blends as compared to the individual components. PCL is a semi-crystalline polymer with lower modulus and higher elongation⁷⁵. Being above the glass transition temperature under ambient conditions, low stress is required to achieve large strain in PCL. PMMA is brittle material with lower elongation and high compressive strength⁷⁶

at room temperature. The mechanical properties of gelatin are closely related to water content⁷⁷. As water content is reduced, it changes gel behavior to rigid polymer. Electrospun gelatin fibers in solid state at ambient conditions have about 10-15% moisture content⁷⁸. Thus, pure gelatin fibers show higher modulus and lower elongation under ambient conditions. Although blends prepared for this study are heterogeneous blends, each component contributes to the improvement of overall mechanical properties. Gelatin plays a modulus boosting role in the blends, whereas PCL enhances the elongation and UTS of the blends. Although we have not measured compressive strength of these blends in this study, we believe all blends would show increase in the compressive modulus due to presence of PMMA.

4.3 DSC and XRD characterization

In order to characterize the nature of the ternary blends and extent of crystallinity present in the polymer sample XRD was performed. Crystalline structure consists of regular arrangement of atoms. Due to the nature of the blended polymers the ternary blends contains both crystalline and amorphous phase arranged randomly. When an X-ray beam is passed through the polymer sample, some of the regularly arranged atoms reflect the x-ray beam constructively and produce enhanced intensified diffraction pattern. Crystalline regions in the polymer seated in well-defined manner acts as diffraction grating.

DSC is another technique to measure crystallinity. The amount of heat absorbed or evolved from sample under isothermal conditions is measured. DSC consists of two pans, one reference pan that is empty and the other pan has polymer sample. In this method polymer sample is heated with reference to a reference pan at the same rate. The amount of extra heat absorbed by polymer sample is measured with reference to reference material.



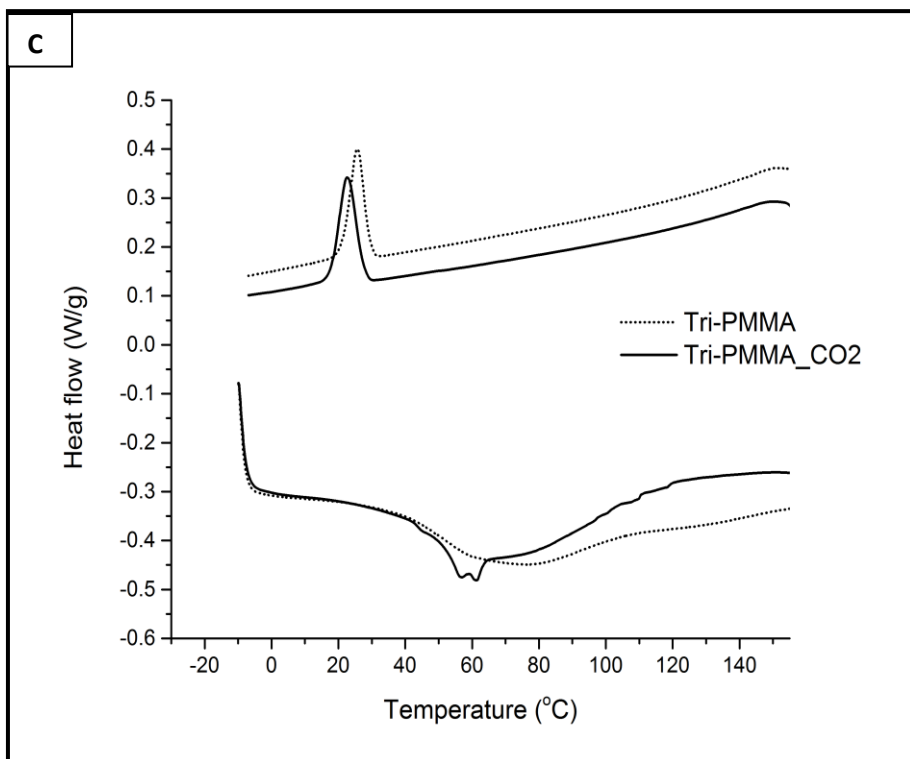
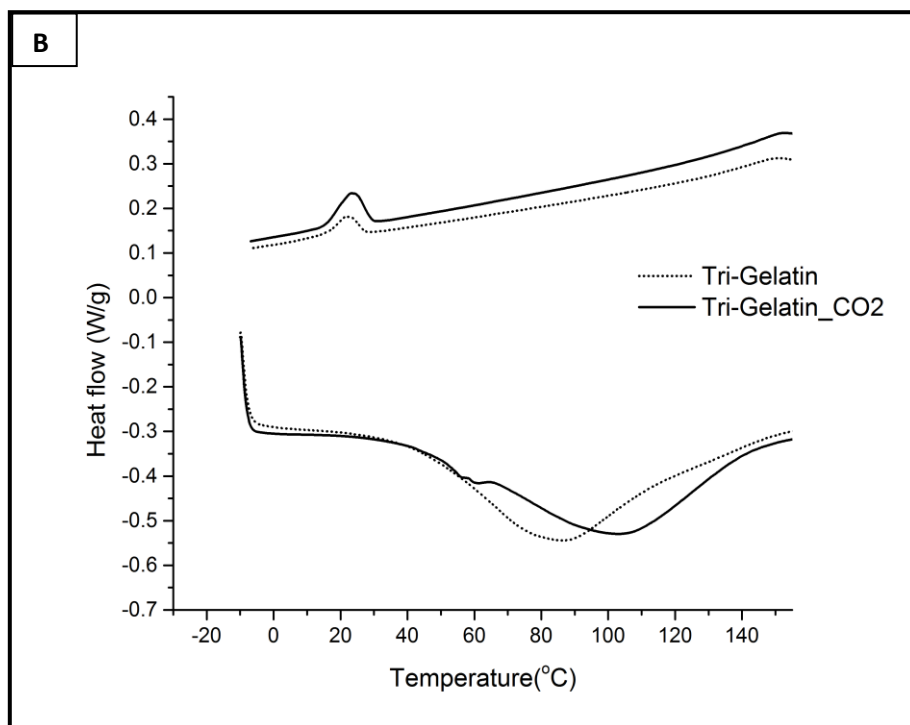


Figure 10: DSC scans of ternary blends as-spun and after supercritical CO₂ (8.27 MPa and 37°C) treatment. Image (A) Tri-PCL (B) Tri-Gelatin (C) Tri-PMMA.

Figure 10 (A-C) shows DSC scans for ternary blends. In the case of untreated samples, a PCL melting peak was observed at 55°C only for Tri-PCL blend (figure 9A). No PCL melting peaks were observed for Tri-Gelatin and Tri-PMMA blends (figure 9B & 9C). In the case of supercritical CO₂ treated samples, all three compositions show PCL melting peaks. A peak splitting phenomenon is observed for all CO₂ treated samples.

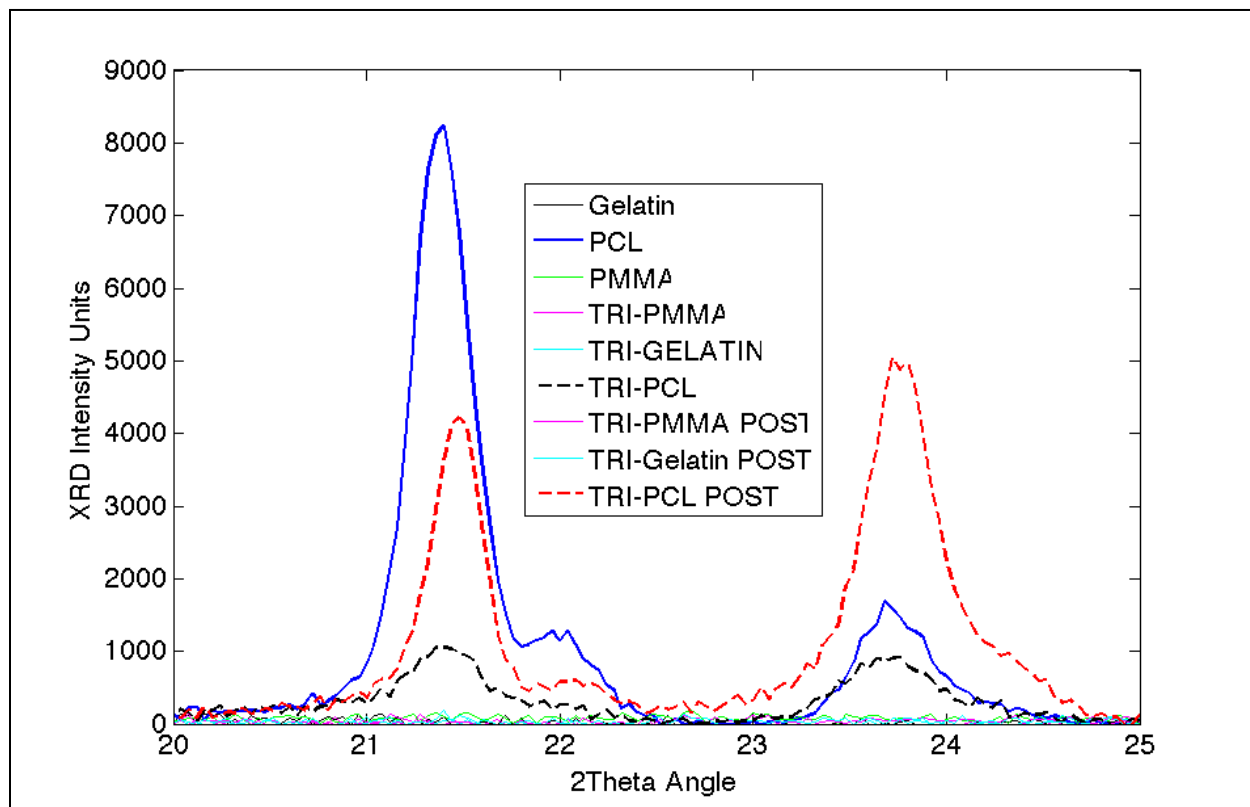


Figure 11: XRD patterns of pure PCL, PMMA and gelatin along with ternary blends before and after CO₂ exposure.

Figure 11, displays the XRD patterns for the as-spun pure-PCL, gelatin, and PMMA samples and ternary blends. The electrospun pure-PCL sample displays significant peaks at 21.5 and 23.75° 2θ, suggestive of a well-defined crystal structure. While, pure-gelatin and PMMA samples display patterns absent of peaks indicating that they are fully amorphous materials. Likewise, the TRI-PMMA and TRI-gelatin three component blends displayed XRD profiles like that of pure-

gelatin and PMMA electrospun samples. The TRI-PCL blended sample displayed peaks at 21.5 and 23.75° 2 θ of lower intensity as compared to the pure-PCL sample, but in the same location, indicating that crystals were formed due to the increased presence of PCL in the blend.

DSC and XRD results suggest that PCL is not in the crystalline form in the Tri-Gelatin and Tri-PMMA blends. However, it shows crystalline phase in the Tri-PCL blend. Further investigation shows that this phenomenon is not related to lower concentration of the PCL in the other two blends. Upon exploring DSC behavior of different compositions of PCL-PMMA and PCL-Gelatin binary blends, a distinct PCL melting peak was observed for all the compositions including compositions having 25% v/v of PCL in the binary blends. Apparently PCL cannot crystallize in the ternary blend in the presence of PMMA and gelatin when concentration is 25% v/v. This suggests that crystallization of PCL is hindered during rapid electrospinning process by rigid gelatin and amorphous PMMA. However, SCCO₂ treated samples show peaks near the melting point of PCL. Thus PCL in the ternary blend is melted and recrystallized after SCCO₂ treatment.

Post processing of electrospun scaffolds is essential before the final applications. Incorporation of drugs or proteins in the scaffolds is accompanied by using solvents which aid in achieving homogeneous distribution of drug. In this study, ethanol was used, since it is a non-solvent for all three polymers and has significant solubility for most of the pharmaceutical drugs. However, diffusion of ethanol through gelatin and PMMA causes stress relaxation of these polymers^{79, 80}. It has been proved experimentally that crystallinity affects the stress relaxation of polymers by inhibiting conformational changes due to presence of rigid crystalline regions⁸¹. This confirms that crystallinity of PCL dominates over stress relaxation behavior of gelatin and PMMA in the Tri-PCL blend and assists in maintaining the fiber structure after ethanol treatment. However, for

Tri-PMMA and Tri-Gelatin, PCL is a minor component in the blend. Also DSC and XRD confirm that PCL is in amorphous form in Tri-Gelatin and Tri-PMMA blends. Due to lack of crystalline PCL, these blends show significant changes in morphology after stress relaxation in ethanol. SCCO₂ is compatible with polymers containing ester groups⁸². PCL melts under supercritical CO₂ whereas PMMA undergoes deformation^{70,83} due to favorable interactions and high CO₂ solubility. Thus, Tri-PMMA blend shows stress relaxation behavior when subjected to supercritical CO₂ and Tri-PCL blend shows melting of fibers at cross sections. However, pure gelatin shows compression when subjected to high pressure CO₂ and assists in retaining the fiber structure in the blend when treated with CO₂. Fiber morphology is still maintained in the Tri-PCL blend post CO₂ treatment due to presence of gelatin and PMMA which aids in maintaining the structure.

4.4 Release of Rhodamine-B

In order to assess the effect of blend composition on the infusion and release of small molecules, the ternary blends were infused with Beta Rhodamine using supercritical CO₂, subcritical CO₂ and simple adsorption. Figure 11 depicts cumulative release curves for various ternary blends.

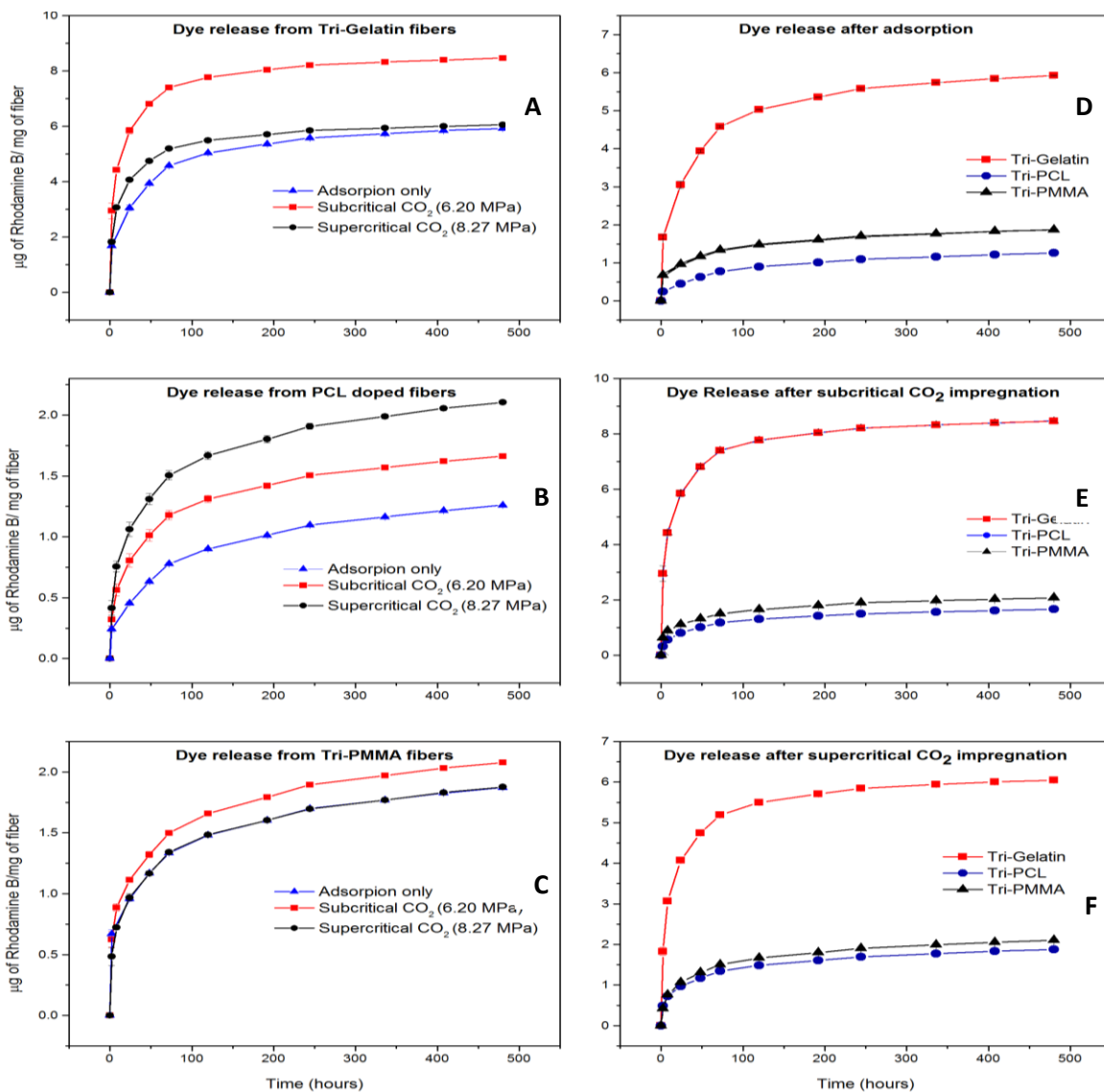


Figure 12: Cumulative release curves of ternary blends under different impregnation conditions
A) Tri-Gelatin B) Tri-PCL C) Tri-PMMA D) Adsorption E) Subcritical CO₂ F) Supercritical CO₂

Release from the blended electrospun fiber mats is shown in figure 11. All release curves are indicated in terms of cumulative mass of Rhodamine B per unit mass of fiber in order to compare different blends and different impregnation conditions.

Figure 11A shows release from Tri-Gelatin fibers impregnated under different infusion conditions. Subcritical CO₂ impregnation releases significantly more dye with time than simple adsorption and supercritical CO₂ impregnated samples. However, samples infused using supercritical CO₂ have a very similar release profile to samples infused by simple adsorption process. This trend may be attributed to the lower degree of dehydration and consequently lower compression of gelatin under subcritical infusion conditions. This in turn allows higher drug loading and release of Rhodamine B from tri-gelatin blends treated with subcritical CO₂.

The Release curves from Tri-PCL fibers (Figure 11B) exhibit an expected trend for mass of dye released. Supercritical CO₂ infusion provides higher loading and release of Rhodamine B than subcritical CO₂ treatment which in turn provides higher impregnation of the dye than a simple adsorption procedure.

In the case of Tri-PMMA fibers (Figure 11C), all three impregnation conditions show similar release profiles without notable change. Subcritical CO₂ impregnated samples show a small but not prominent increase in the amount of released dye as compared to supercritical CO₂ and adsorption. The most likely explanation for this abnormal behavior is lower diffusion of release medium in the Tri-PMMA samples due to reduction in void volume. Also subcritical CO₂ and supercritical CO₂ show similar swelling for PMMA when subjected below 40°C⁸⁴.

Figures 11D-F show comparative release profiles of all ternary blends subjected to identical impregnation conditions. Under all the infusion conditions tri-gelatin shows the highest release followed by tri-PMMA and finally tri-PCL.

The results confirm that each polymer in the blend can show a unique response towards solute release based on the polymer solute interactions and impregnation conditions⁸⁵. Additionally, degradation of the polymer matrix due to hydrolysis and morphology changes upon exposure to release medium can affect release of solute⁸⁶.

If we consider solute polymer interactions for ternary blends, solubility parameters for different polymers with Rhodamine B can provide a basis for comparison^{87- 90}. Solubility parameters of PCL, PMMA and gelatin are 18.25, 18.2 and 24.3 MPa^{0.5} respectively. Solubility parameter of Rhodamine B calculated from group contribution theory is about 27.4 MPa^{0.5}. Thus, gelatin should have higher compatibility for Rhodamine B as compared to PCL and PMMA. This may explain higher release of dye from tri-gelatin blend under all the different impregnation conditions. The higher compatibility of Rhodamine-B with the gelatin component of polymer matrix, allows for enhanced drug loading. This allows higher release of dye from tri-gelatin irrespective of impregnation conditions.

Relaxation dynamics of polymers play an important role in the impregnation and release. Tri-PMMA and Tri-gelatin electrospun fibers in their pure state show prominent reduction in the voidage of electrospun mat when subjected to 100% ethanol. This phenomenon is explained by relaxation of stresses built up during rapid electrospinning process. As shown in the SEM analysis (Figure 1B and 1C), both Tri-PMMA and Tri-Gelatin blends show decrease in the free volume of an electrospun mat when subjected to Rhodamine B in ethanol. For Tri-gelatin fibers, a large degree of melting was observed, whereas, Tri-PMMA fibers show no melting but reduction in the void volume and change in fiber structure. Tri-PCL scaffolds show no change in structure after pure ethanol wetting. This explains why different impregnation conditions have significant impact on the release of dye from tri-PCL blends since fiber morphology is relatively

resistant to stress relaxation. However, in case of tri-PMMA fibers the impregnation conditions only show a modest effect on the release of dye. Moreover % release curves for tri-PMMA shown in Figure 13 C show that rate of dye released is also nearly unaffected for different impregnation conditions. This confirms that release from Tri-PMMA scaffolds is controlled dominantly by the diffusion of solvent medium in the scaffold.

In order to view time related release behavior % release curves were plotted in Figure 13. The cumulative dye released at each time point was expressed as a percentage of the final cumulative amount of dye released at termination of the release period.

As is evident from Figure 13E and F, tri-gelatin fibers shows the highest burst release with 50% of total dye being diffused within 24 hours. Also, Figures 13A-C depicts near linear release curves from 50% of total dye released onwards for all three ternary blends. The linear release of dye with time may be significant for controlled release applications. Release curves for tri-PCL and tri-gelatin blends (Figures 13A-B) exhibit that CO₂ treatment has a significant impact on the rate of release.

Finally the polymers differ in their stability in the aqueous release medium. PMMA is non-biodegradable polymer which cannot be degraded hydrolytically⁹¹. PCL, a poly-hydroxy ester, shows slow hydrolysis of ester groups in PBS which proceeds via surface as well as bulk degradation of PCL.⁹² Uncrosslinked gelatin is extremely unstable in aqueous media and shows rapid degradation of polymer matrix. Thus higher release of tri-gelatin blend may be explained by the direct degradation of the polymer-solute complex into the aqueous release media. The results of the weight loss with time in PBS release medium are shown in Figure 14.

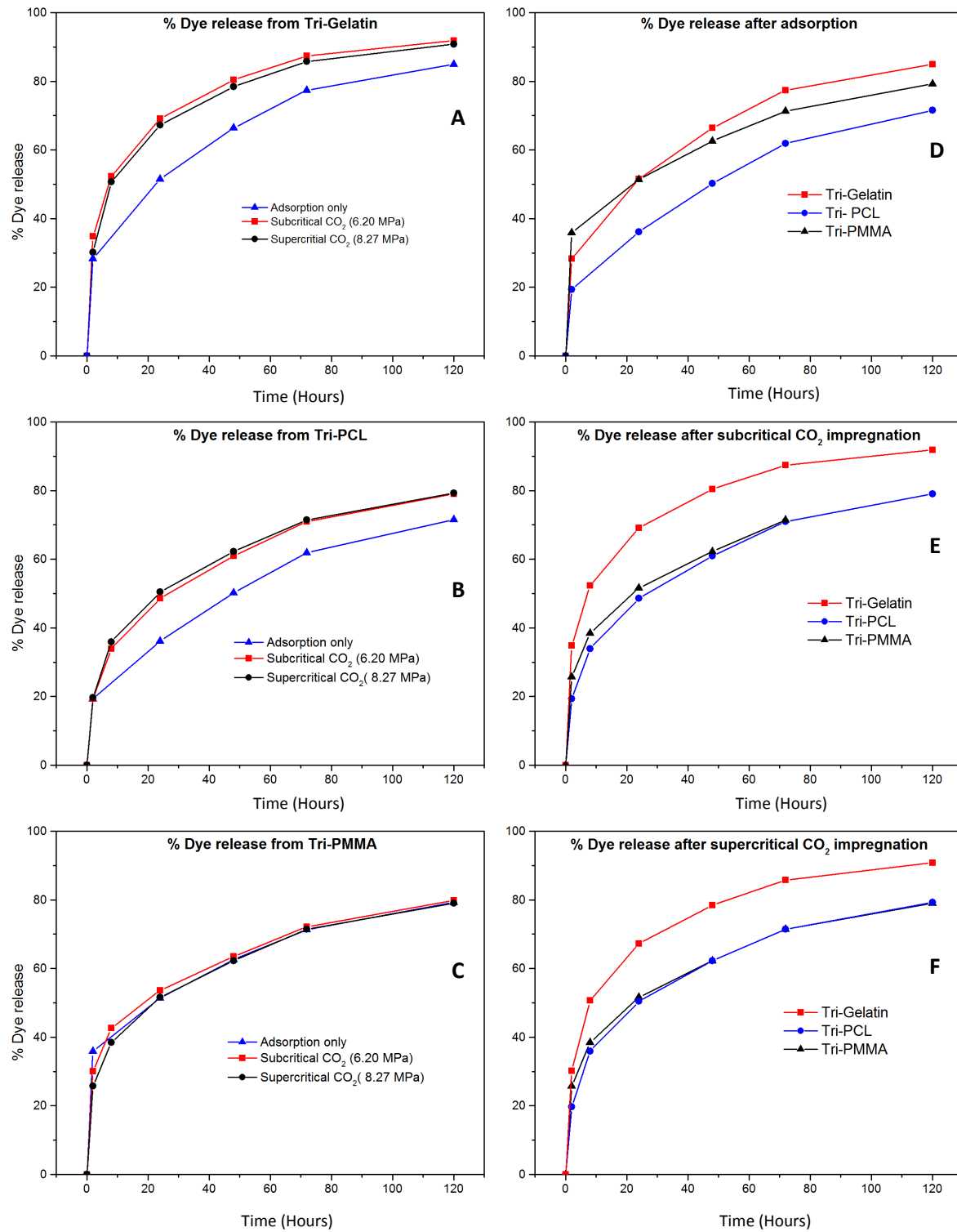


Figure 13: Comparison of % dye release profiles from ternary blends after different impregnation conditions for initial 5 days of release

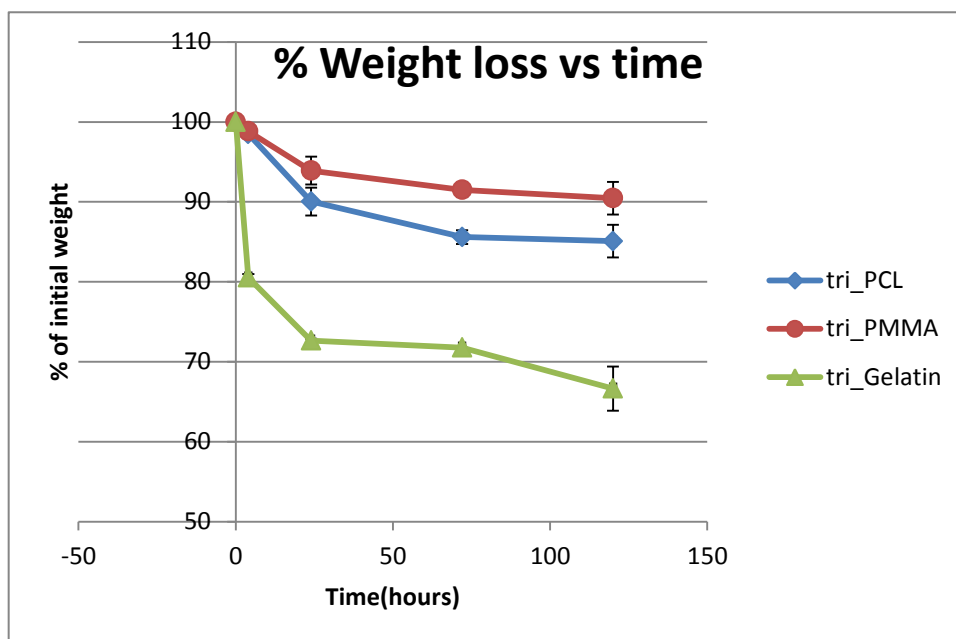


Figure 14: Degradation of ternary electrospun scaffolds in PBS release medium

The results show rapid degradation of tri-gelatin fibers by direct hydrolysis of the gelatin component of the polymer matrix. Similarly the tri-PCL and tri-PMMA blends show weight loss in PBS, although the tri-PCL blend shows more rapid weight loss as compared to tri-PMMA. This could be attributed to the fact that tri-PCL fibers maintain void volume in PBS and allow for more rapid diffusion of solvent into the polymer matrix, thus allowing for faster degradation of the gelatin component into the solvent. The SEM images of tri-blends after exposure to PBS are shown in Figure 15.

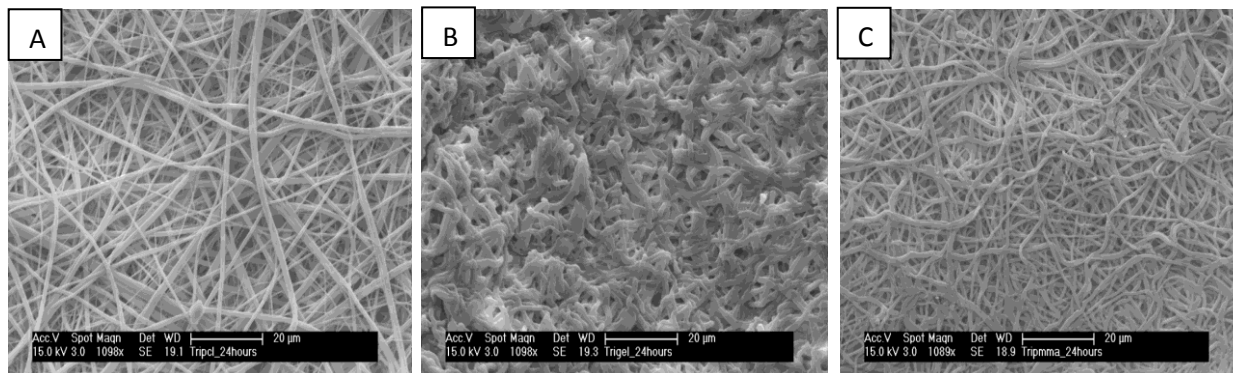


Figure 15: SEM images of as-spun ternary blends after 24 hour of degradation in PBS (A) Tri-PCL (B) Tri-Gelatin (C) Tri-PMMA.

If we model these scaffolds by considering a thin film, we can calculate fickian diffusion coefficients of dye release using procedure explained by⁹³ Ritger et.al.. Diffusion coefficients (Table 1) indicate that all three compositions have different limiting factors in the release of dye. Tri-PMMA fibers show slowest release with lowest diffusion coefficients. This is the result of formation of fibrous membrane of Tri-PMMA scaffolds after stress relaxation. Since Tri-PCL scaffolds can maintain the porosity during the release (Figure 15 A), higher diffusion coefficients were obtained. In the case of Tri-Gelatin fibers, rapid dissolution of gelatin releases dye quickly as compared to Tri-PCL and Tri-PMMA scaffolds.

	$D_{\text{Tri-PCL}}$ (mm ² /sec)	$D_{\text{Tri-PMMA}}$ (mm ² /sec)	$D_{\text{Tri-Gelatin}}$ (mm ² /sec)
Adsorption	6.9×10^{-10}	4.8×10^{-10}	9.3×10^{-10}
Subcritical 900	9.92×10^{-10}	6.4×10^{-10}	18.4×10^{-10}
Supercritical 1200	9.85×10^{-10}	7.7×10^{-10}	20.6×10^{-10}

Table 1: Diffusion coefficients of Rhodamine B from ternary blends infused using different impregnation conditions in a static release medium (PBS).

5. Conclusion:

In this study, simple electrospinning procedure was used to prepare ternary blend scaffolds of Tri-PCL (PCL 50%, PMMA 25%, Gelatin 25%), Tri-PMMA (PCL 25%, PMMA 50%, Gelatin 25%) and Tri-Gelatin (PCL 25%, PMMA 25%, Gelatin 50%) blends. Blending of the three polymers and changing blend composition lends unique properties to the resultant electrospun scaffolds. PCL boosts the elongation capacity of the blend and aids in maintaining structural properties during further processing of blend. Gelatin imparts higher modulus and capability to achieve rapid release of the impregnated drug. Additionally, it makes the blend bioactive and allows efficient adhesion of proteins and cells. PMMA contributes in compressive strength of scaffold and allows longer degradation period. Stress relaxation of PMMA fibers lead to loss of fiber porosity. However, it maintains the fiber structure and thus has high surface area. This has potential for use in dermal and transdermal patches for long term drug delivery.

CO₂ assisted impregnation allows control over loading and release rates. Adjusting composition of PMMA-PCL-gelatin ternary blend and tuning impregnation condition several tissue engineered scaffolds and controlled drug delivery systems can be designed for efficient biomedical applications. Composition of the ternary blend was found to be a vital component in deciding several properties of these electrospun scaffolds. Significant improvement was obtained in the mechanical properties of ternary blends as compared to individual components of the blend. DSC and XRD studies show noteworthy changes in the crystalline properties of PCL in the ternary blend, rendering them better suited for impregnation of additives.

CO₂ assisted impregnation of drugs and biomolecules in polymers is trouble free, benign and ‘green’ alternative to current impregnation processes. A dye release study was carried out from all three blend compositions under various impregnation conditions. Stress relaxation of PMMA

and gelatin in the presence of ethanol during impregnation process changes morphological properties of Tri-PMMA and Tri-Gelatin blend but Tri-PCL remains unchanged due to high crystalline content. Three measure factors were found to have significant impact on the dye release profiles from ternary blends: 1) Impregnation treatment of CO₂ 2) degradation rate of scaffold 3) Porosity of scaffold. Tri-PCL blend have long degradation rate and maintains porosity of the scaffold in the release medium. Effect of CO₂ was dominant in the case of Tri-PCL blends. For Tri-Gelatin scaffolds, degradation rate was found to be key factor in rapid release of the dye from scaffolds. Also ethanol treatment shows significant melting of Tri-Gelatin fibers which increases the loading of the dye in the blend. In the case of Tri-PMMA, stress relaxation in the presence of ethanol reduces the porosity of the scaffold. Although PMMA shows increase in swelling under high pressure CO₂, release of Rhodamine B is limited by porosity of the scaffold and diffusion of release medium in the scaffold. In summary, all three polymers show unique contribution in altering the properties of the ternary blends. Different blend ratios can be used to tune the characteristics of the blend and prepare several platforms to fulfill needs of biomedical engineering.

6. Recommendations for future work:

Blend optimization has shown some promise in altering properties of the electrospun scaffolds. Further exploration via changing blend composition may yield interesting results in terms of mechanical properties, resilience to high pressure CO₂ impregnation, resistance to stress relaxation of polymer matrix during post fabrication processing, and loading and release characteristics.

The current tri-PMMA and tri-gelatin scaffolds show microstructure deformation during several post fabrication processing conditions. Thermal and chemical crosslinking has been proven to be successful in providing resistance to microstructural deformation. This may open up vistas for further controlling the release and degradation of tri-PMMA and tri-Gelatin blends.

In this study only the release of Rhodamine – B was tested for controlled release applications. The solute – polymer interactions calculated via group contribution theory confirm that Rhodamine –B has higher affinity for gelatin. This may be a confounding factor in assessing the release characteristics of ternary blends. A more comprehensive release study is required, which uses different additive molecules to better assess the efficacy of the loading and release characteristics of the ternary blends.

Finally to assess tissue engineering aspects of the scaffolds a cellular adhesion study is required to measure quantitative and qualitative aspects of cellular proliferation on the scaffolds. This will allow fine tuning of scaffold properties and post fabrication processing conditions to generate viable surrogates for the extracellular matrix (ECM), provide mechanical stability, and assist in directing cellular activity.

7. Acknowledgements:

I would like to sincerely thank the college of Engineering at the Ohio State University for their support. I would like to express my gratitude towards my research advisor Dr. David L. Tomasko for allowing me the opportunity to join the research group and receive invaluable experience. Additionally, I would like to thank Dr. Jeffrey J. Chalmers for his willingness to be on my thesis committee. Finally, I would like to thank Hrishikesh R. Munj and Mark Tyler Nelson for their sincere guidance and patient mentorship.

References:

1. Colton, J.S., and Suh, N.P. Nucleation of microcellular foam: theory and practice. *Polym Eng Sci* 27, 500, 1987.
2. Nalawade, S.P., F. Picchioni, and L.P.B.M. Janssen, "Supercritical carbon dioxide as a green solvent for processing polymer melts: Processing aspects and applications". *Progress in Polymer Science*, 2006. 31(1): p. 19.
3. Ramsey, E., et al., "Mini-Review: Green sustainable processes using supercritical fluid carbon dioxide". *Journal of Environmental Sciences*, 2009. 21(6): p. 720.
4. Collins, N.J., Bridson, R.H., Leeke, G.A., and Grover, L.M. Particle seeding enhances interconnectivity in polymeric scaffolds foamed using supercritical CO₂. *Acta Biomater* 6, 1055, 2010.
5. White, L.J., Hutter, V., Tai, H., Howdle, S.M., and Shakesheff, K.M. The effect of processing variables on morphological and mechanical properties of supercritical CO₂ foamed scaffolds for tissue engineering. *Acta Biomater* 8, 61, 2012.
6. Reverchon, E., and Cardea, S. Supercritical fluids in 3-D tissue engineering. *J Supercrit Fluids* 69, 97, 2012.
7. Davies, O.R., Lewis, A.L., Whitaker, M.J., Tai, H., Shakesheff, K.M., and Howdle, S.M. Applications of supercritical CO₂ in the fabrication of polymer systems for drug delivery and tissue engineering. *Adv Drug Deliv Rev* 60, 373, 2008.
8. Tai, H., Popov, V.K., Shakesheff, K.M., and Howdle, S.M. Putting the fizz into chemistry: applications of supercritical carbon dioxide in tissue engineering, drug delivery and synthesis of novel block copolymers. *Biochem Soc Trans* 35, 516, 2007.
9. Barry, J.J., Silva, M.M., Popov, V.K., Shakesheff, K.M., and Howdle, S.M. Supercritical carbon dioxide: putting the fizz into biomaterials. *Philos Trans Ser A Math Phys Eng Sci* 364, 249, 2006.
10. Kazarian, S.G., et al., "Specific Intermolecular Interaction of Carbon Dioxide with Polymers". *Journal of the American Chemical Society*, 1996. 118(7): p. 1729.
11. Nalawade, S.P., et al., "The FT-IR studies of the interactions of CO₂ and polymers having different chain groups". *The Journal of Supercritical Fluids*, 2006. 36(3): p. 236.
12. Levit, N., and Tepper, G. Supercritical CO₂-assisted electrospinning. *J Supercrit Fluids* 31, 329, 2004.
13. Ayodeji, O., Graham, E., Kniss, D., Lannutti, J., and Tomasko, D. Carbon dioxide impregnation of electrospun polycaprolactone fibers. *J Supercrit Fluids* 41, 173, 2007.
14. Li, D., and Xia, Y. Electrospinning of nanofibers: reinventing the wheel? *Adv Mater* 16, 1151, 2004.
15. Sato, Y., et al., "Solubility and Diffusion Coefficient of Carbon Dioxide in Biodegradable Polymers". *Industrial & Engineering Chemistry Research*, 2000. 39(12): p. 4813.
16. Davies, O.R., et al., "Applications of supercritical CO₂ in the fabrication of polymer systems for drug delivery and tissue engineering". *Advanced Drug Delivery Reviews*, 2008. 60(3): p. 373.
17. Nelson, M., Munj, H., Tomasko, D., & Lannutti, J. (2012). Carbon dioxide infusion of composite electrospun fibers for tissue engineering. *Journal of Supercritical Fluids*, 70(2012), 90-99.
18. Diankov, S., & Barth, D. (n.d.). Supercritical impregnation isotherm of o-hba on pmma in batch stirred reactor. Unpublished manuscript, Dept. Eng. Chemistry, System and

Chemical Engineering Faculty, University of Chemical Technology and Metallurgy, Sofia, Bulgaria.

19. Sachlos, E., & Czernuszka, J. U.S. National Library of Medicine, (2003). Making tissue engineering scaffolds work. review: the application of solid freeform fabrication technology to the production of tissue engineering scaffolds. *European cells & materials*, 2003 Jun 30; 5: 29-39; discussion 39-40.
20. Meinel, A., & Gernershaus, O. (2012). Electrospun matrices for localized drug delivery: Current technologies and selected biomedical applications. *European Journal of Pharmaceutics and Biopharmaceutics*, 81(1), 1-13.
21. Zeng, J., & Xu, X. (2003). Biodegradable electrospun fibers for drug delivery. *Journal of Controlled Release*, 92(3), 227-231.
22. Grodzinski, J. (2006). Polymers for tissue engineering, medical devices, and regenerative medicine. concise general review of recent studies. *POLYMERS FOR ADVANCED TECHNOLOGIES*, doi: 10.1002
23. Gloria, A., Ambrosio, L., & De Santis, R. (2010). Polymer-based composite scaffolds for tissue engineering. *Journal of Applied Biomaterials & Biomechanics*, 8(2), 57-67.
24. Place, E., & George, J. (2009). Synthetic polymer scaffolds for tissue engineering. *Chemical Society Review*, 38(4), 1139-1151. doi: 10.1039/B811392K
25. Ulery, B., & Nair, L. (2011). Biomedical applications of biodegradable polymers. *JOURNAL OF POLYMER SCIENCE*, doi: 10.1002/polb.22259
26. Lam, C., & Hutmacher, D. (2008). Evaluation of polycaprolactone scaffold degradation for 6 months in vitro and in vivo. *Journal of Biomedical Materials Research*, doi: 10.1002/jbm.a.32052
27. Sun, H., et al., "The in vivo degradation, absorption and excretion of PCL-based implant". *Biomaterial*, 2006. 27(9): p. 1735.
28. Shea, L.D., Wang, D., Franceschi, R.T., Mooney, D.J. Engineered bone development from a pre-osteoblast cell line on
29. Mao J, Zhao L, De Yao K, Shang Q, Yang G, Cao Y. Study of novel chitosan-gelatin artificial skin in vitro. *J Biomed Mater Res* 2003;64A:301-8.
30. J. Venugopal, L.L. Ma, T. Yong, S. Ramakrishna, In vitro study of smooth muscle cells on polycaprolactone and collagen nanofibrous matrices, *Cell Biology International* 29 (2005) 861-867.
31. J. Mey, E. Schnell, K. Klinkhammer, S. Balzer, G. Brook, D. Klee, P. Dalton, Guidance of glial cell. Migration and axonal growth on electrospun nanofibers of poly-epsilon-caprolactone and a collagen/poly-epsilon-caprolactone blend, *Biomaterials* 28 (2007) 3012-3025.
32. Peppas NA, Langer R. *Science* 1994;263:1715e20.
33. Marchant RE, Wang I. In: Greco RS, editor. *Implantation biology: the host response and biomedical devices*. CRC Press; 1994. p. 13e38.
34. Wei, S., & Sampathi, J. (2011). Nanoporous poly(methyl methacrylate)-quantum dots nanocomposite fibers toward biomedical applications. *Polymer*, 52(25), 5817-5829.
35. Zhang, F., & Sun, F. (2005). Measurement of cell motility on proton beam micromachined 3d scaffolds. *Nuclear Instruments and Methods in Physics Research Section B: Beam Interactions with Materials and Atoms*, 231(1-4), 413-418.
36. Srouji, S., & Kizhner, T. (2006). 3d scaffolds for bone marrow stem cell support in bone repair. *Regenerative Medicine*, 1(4), 519-528. doi: 10.2217/17460751.1.4.519

37. Shi, M., & Kretlow, J. (2011). Antibiotic-releasing porous polymethylmethacrylate/gelatin/antibiotic constructs for craniofacial tissue engineering . *Journal of Controlled Release*, 52(1), 196–205.
38. Liu, X., & Holzwarth, J. (2012). Functionalized synthetic biodegradable polymer scaffolds for tissue engineering. *Macromolecular bioscience*, 12(7), 911-919.
39. Liu, X., & Won, Y. (2006). Porogen-induced surface modification of nano-fibrous poly(l-lactic acid) scaffolds for tissue engineering. *Biomaterials*, 27(21), 3980–3987. doi: 10.1016/j.biomaterials.2006.03.008
40. Liu, X., & Won, Y. (2005). Surface modification of interconnected porous scaffolds. *Journal of Biomedical Materials Research*, 27(21), 3980-3987. doi: 10.1002/jbm.a.30367
41. Hubbell, J. (1995). Biomaterials in tissue engineering. *Nature Biotechnology*, doi: 10.1038/nbt0695-565
42. Liu, W., & Chen, C. (2005). Engineering biomaterials to control cell function. *Materials Today*, 8(12), 28-35.
43. Almine, J., & Bax, D. (2010). Elastin-based materials. *Chemical Society Review*, doi: 10.1039/B919452P
44. Li M, Mondrinos MJ, Gandhi MR, Ko FK, Weiss AS, Lelkes PI. Electrospun protein fibers as matrices for tissue engineering. *Biomaterials* 2005;26:5999–6008.
45. Barbani, N.; Lazzeri, L.; Cristallini, C.; Cascone, M. G.; Polacco, G.; Pizzirani, G. J. *Appl. Polym. Sci.* **1999**, 72, 971-976.
46. Cascone, M. G.; Polacco, G.; Lazzeri, L.; Barbani, N. J. *Appl. Polym. Sci.* **1997**, 66, 2089-2094.
47. Giusti, P.; Lazzeri, L.; De Petris, S.; Palla, M.; Cascone, M. G. *Biomaterials* **1994**, 15, 1229-1233.
48. Cascone, M. G.; Di Pasquale, G.; La Rosa, A. D.; Cristallini, C.; Barbani, N.; Recca, A. *Polymer* **1998**, 39, 6357-6361.
49. Edlund, U., & Albertsson, A. (2000). Sterilization, storage stability and in vivo biocompatibility of poly(trimethylene carbonate)/poly(adipic anhydride) blends. *Biomaterials*, 21(9), 945-955.
50. Cascone, M. G.; Barbani, N.; Cristallini, C.; Giusti, P.; Ciardelli, G.; Lazzeri, L. J. *Biomater. Sci. Polym. Ed.* **2001**, 12, 267-281.
51. Li, M., & Mondrinos, M. (2006). Co-electrospun poly(lactide-co-glycolide), gelatin, and elastin blends for tissue engineering scaffolds. *Journal of Biomedical Materials Research*, 79(4), 963-973. doi: 10.1002/jbm.a.30833
52. E.D. Boland, K.J. Pawlowski, C.P. Barnes, D.G. Simpson, G.E. Wnek, G.L. Bowlin, Electrospinning of bioresorbable polymers for tissue engineering scaffolds, *ACS Symposium Series* 918 (2006) 188–204.
53. Y.Z. Zhang, Electrospinning of gelatin fibers and gelatin/PCL composite fibrous scaffolds, *J. Biomedical Material Research B* 72B (2005) 156–165.
54. Y.Z. Zhang, J. Venugopal, Z.M. Huang, C.T. Lim, S. Ramakrishna, Characterization of the surface biocompatibility of the electrospun PCL–collagen nanofibers using fibroblasts, *Biomacromolecules* 6 (2005) 2583–2589
55. B.S. Hsiao, D. Liang, B. Chu, Functional electrospun nanofibrous scaffolds for biomedical applications, *Advanced Drug Delivery Review* 59 (2007) 1392–1412.

56. G. Bowlin, S. Sell, C. Barnes, M. Smith, M. McClure, P. Madurantakam, J. Grant, M. Mcmanus, Extracellular matrix regenerated: tissue engineering via electrospun biomimetic nanofibers, *Polymer International* 56 (2007) 1349–1360.
57. A.G.A. Coombes, E. Verderio, B. Shaw, X. Li, M. Griffin, S. Downes, Biocomposites of non-crosslinked natural and synthetic polymers, *Biomaterials* 23 (2002) 2113–2118.
58. S.L. Cooper, D.E. Heath, J.J. Lannutti, Electrospun scaffold topography affects endothelial cell proliferation, metabolic activity, and morphology, *J. Biomedical Materials Research A* 94A (2010) 1195–1204.
59. N.T. Dai, M.R. Williamson, N. Khammo, E.F. Adams, A.G.A. Coombes, Composite cell support membranes based on collagen and polycaprolactone for tissue engineering of skin, *Biomaterials* 25 (2004) 4263–4271.
60. H.L. Khor, K.W. Ng, J.T. Schantz, T.T. Phan, T.C. Lim, S.H. Teoh, D.W. Hutmacher, Poly(epsilon-caprolactone) films as a potential substrate for tissue engineering an epidermal equivalent, *Material Science Engineering C-Bio S* 20 (2002) 71–75.
61. J. Venugopal, Y.Z. Zhang, S. Ramakrishna, Fabrication of modified and functionalized polycaprolactone nanofibre scaffolds for vascular tissue engineering, *Nanotechnology* 16 (2005) 2138–2142.
62. J.R. Venugopal, Y.Z. Zhang, S. Ramakrishna, In vitro culture of human dermal fibroblasts on electrospun polycaprolactone collagen nanofibrous membrane, *Artificial Organs* 30 (2006) 440–446.
63. Alvarez-Perez, M., & Guarino, V. (2010). Influence of gelatin cues in pcl electrospun membranes on nerve outgrowth. *Biomacromolecules*, 11(9), 2238-46.
64. Young, S., & Wong, M. (2005). Gelatin as a delivery vehicle for the controlled release of bioactive molecules. *Journal of Controlled Release*, 109(1-3), 256–274.
65. Duarte, A., & Mano, J. (2009). Supercritical fluids in biomedical and tissue engineering applications: a review. *International Materials Reviews*, 54(4), 214-222.
66. Cooper, A. (2000). Polymer synthesis and processing using supercritical carbon dioxide. *Journal of Materials Chemistry*, doi: 10.1039/A906486I
67. Nalawade, S., & Picchioni, F. (2006). Supercritical carbon dioxide as a green solvent for processing polymer melts: Processing aspects and applications. *Progress in Polymer Science*, 31(1), 19-43.
68. Kazarian, S., & Vincent, M. (1996). Specific intermolecular interaction of carbon dioxide with polymers. *Journal of the American Chemical Society*, doi: 10.1021/ja950416q
69. Tomasko, D., Hongbo, L., Lee, J., & Koelling, K. (2003). A review of co2 applications in the processing of polymers. *Industrial and Engineering Chemistry Research*, 42(25), 6431–6456. doi: 10.1021/ie030199z
70. Shieh, Y., & Yang, H. (2005). Morphological changes of polycaprolactone with high-pressure co2 treatment. *Journal of Supercritical Fluids*, 33(2), 183–192.
71. Goel, S., & Beckman, E. (1993). Plasticization of poly(methyl methacrylate) (pmma) networks by supercritical carbon dioxide. *Polymer*, 34(7), 1410–1417.
72. Ayodeji, O., Graham, E., Lannutti, J., & Tomasko, D. (2007). Carbon dioxide impregnation of electrospun polycaprolactone fibers. *Journal of Supercritical Fluids*, 41(1), 173–178.
73. Kamiya, Y., & Mizoguchi, K. (1998). Co2 sorption and dilation of poly(methyl methacrylate). *Macromolecules*, 31(2), 472-478. doi: 10.1021/ma970456

74. Gu, S., Wang, Z. (2009). Electrospinning of gelatin and gelatin/poly(l-lactide) blend and its characteristics for wound dressing. *Materials Science and Engineering*, 29(6), 1822–1828.
75. Tan, E. P. S., & Lim, C. T. (2005). Tensile testing of a single ultrafine polymeric fiber. *Biomaterials*, 26(13), 1453–1456.
76. Mousa, W., & Kobayashi, M. (2000). Biological and mechanical properties of pmma-based bioactive bone cements. *Biomaterials*, 21(21), 2137–2146.
77. Yakimets, I., & Wellner, N. (2005). Mechanical properties with respect to water content of gelatin films in glassy state. *Polymer*, 46(26), 12577–12585.
78. Zhang, Y. Z., & Venugopal, J. (2006). Crosslinking of the electrospun gelatin nanofibers. *Polymer*, 47(8), 2911–2917.
79. Jopling, D. W. (2003). Stress relaxation studies of chemically crosslinked gelatin films. *JOURNAL OF POLYMER SCIENCE*, 3(2), 513–526. doi: 10.1002/pol.1965.100030210
80. Sarti, G. C., & Gostoli, C. (1983). Diffusion of alcohols and relaxation in poly(methyl methacrylate): effect of thermal history. *Journal of Membrane Science*, 5(2), 181–192.
81. Matthews, R. G., & Aji, A. (2000). The effects of stress relaxation on the structure and orientation of tensile drawn poly(ethylene terephthalate). *Polymer*, 41(19), 7139–7145.
82. Shen, Z., & McHugh, M. A. (2003). Co₂-solubility of oligomers and polymers that contain the carbonyl group. *Polymer*, 44(5), 1491–1498.
83. Liu, D., Li, H., Noon, M., & Tomasko, D. (2005). Co₂-induced pmma swelling and multiple thermodynamic property analysis using sanchez–lacombe eos. *Macromolecules*, 38(10), 4416–4424.
84. Wissinger, R. G., & Paulaitis, M. E. (2003). Swelling and sorption in polymer–co₂ mixtures at elevated pressures. *JOURNAL OF POLYMER SCIENCE*, 25(12), 2497–2510. doi: 10.1002/polb.1987.090251206
85. Kikic, I., & Vecchione, F. (2003). Supercritical impregnation of polymers. *Current Opinion in Solid State and Materials Science*, 7(4-5), 399–405.
86. Freiberg, S., & Zhu, X. X. (2004). Polymer microspheres for controlled drug release. *International Journal of Pharmaceutics*, 282(1-2), 1-18.
87. Varnell, D. F., & Coleman, M. M. (1981). Ft i.r. studies of polymer blends: V. further observations on polyester-poly(vinyl chloride) blends. *Polymer*, 22(10), 1324–1328.
88. Singh, Y. P., & Singh, R. P. (n.d.). Compatibility studies on solutions of polymer blends by viscometric and ultrasonic techniques. *European Polymer Journal*, 19(6), 535–541.
89. Hancock, B., & York, P. (n.d.). The use of solubility parameters in pharmaceutical dosage form design. *International Journal of Pharmaceutics*, 148(1), 1–21.
90. Stefanis, E., & Panayiotou, C. (2008). Prediction of hansen solubility parameters with a new group-contribution method. *International Journal of Thermophysics*, 29(2), 568-585.
91. Shirahase, T., & Komatsu, Y. (2006). Miscibility and hydrolytic degradation in alkaline solution of poly(l-lactide) and poly(methyl methacrylate) blends. *Polymer*, 47(13), 4839–4844.
92. Li, W., & Cooper, J. A. (2006). Fabrication and characterization of six electrospun poly(α -hydroxy ester)-based fibrous scaffolds for tissue engineering applications. *Acta Biomaterialia*, 2(4), 377–385.

93. Ritger, P., & Nikolaos, P. (1987). A simple equation for description of solute release ii. fickian and anomalous release from swellable devices. *Journal of Controlled Release*, 5(1), 37–42.